# Znhit1 Regulates p21$^{Cip1}$ to Control Mouse Lens Differentiation

Juan Lu,[1,2] Jianhong An,[1,2] Jiawei Wang,[1,2] Xiaowen Cao,[1,2] Yuqing Cao,[1,2] Chengjie Huang,[1,2] Shiming Jiao,[1,2] Dongsheng Yan,[1,2] Xinhua Lin,[6] and Xiangtian Zhou[1–5]

[1]School of Optometry and Ophthalmology and Eye Hospital, Wenzhou Medical University, Wenzhou, Zhejiang, China
[2]State Key Laboratory of Optometry, Ophthalmology and Vision Science, Wenzhou, Zhejiang, China
[3]National Clinical Research Center for Ocular Diseases, Wenzhou, China
[4]Oujiang Laboratory, Zhejiang Lab for Regenerative Medicine, Vision and Brain Health, Wenzhou, Zhejiang, China
[5]Research Unit of Myopia Basic Research and Clinical Prevention and Control, Chinese Academy of Medical Sciences, Wenzhou, China
[6]State Key Laboratory of Genetic Engineering, School of Life Sciences, Zhongshan Hospital, Fudan University, Shanghai, China

Correspondence: Xinhua Lin, State Key Laboratory of Genetic Engineering, School of Life Sciences, Zhongshan Hospital, Fudan University, Shanghai 200438, China; xlin@fudan.edu.cn.
Xiangtian Zhou: School of Optometry and Ophthalmology and Eye Hospital, Wenzhou Medical University, 270 Xueyuan Rd, Wenzhou, Zhejiang 325027, China; zxt@mail.eye.ac.cn.

JL and JA contributed equally to this work.

**Received:** December 9, 2021
**Accepted:** April 6, 2022
**Published:** April 26, 2022

Citation: Lu J, An J, Wang J, et al. Znhit1 regulates p21$^{cip1}$ to control mouse lens differentiation. *Invest Ophthalmol Vis Sci.* 2022;63(4):18. https://doi.org/10.1167/iovs.63.4.18

**Purpose.** The transparency of the ocular lens is essential for refracting and focusing light onto the retina, and transparency is controlled by many factors and signaling pathways. Here we showed a critical role of chromatin remodeler zinc finger HIT-type containing 1 (Znhit1) in maintaining lens transparency.

**Methods.** To explore the roles of Znhit1 in lens development, the cre-loxp system was used to generate lens-specific Znhit1 knockout mice (Znhit1$^{Mlr10\text{-}Cre}$; Znhit1 cKO). Morphological changes in mice lenses were examined using hematoxylin and eosin staining. RNA sequencing (RNA-seq) and assay for transposase accessible chromatin using sequencing (ATAC-seq) were applied to screen transcriptome changes. Immunofluorescence staining were performed to assess proteins distribution and terminal deoxynucleotidyl transferase dUTP nick-end labeling staining were used for determining apoptosis. The mRNAs expression was examined by quantitative RT-PCR and proteins expression by Western blot.

**Results.** Lens-specific conditional knockout mice had a severe cataract, microphthalmia phenotype, and seriously abnormal lens fiber cells differentiation. Deletion of Znhit1 in the lens resulted in decreased cell proliferation and increased cell apoptosis of the lens epithelia. ATAC-seq showed that Znhit1 deficiency increased chromatin accessibility of cyclin-dependent kinase inhibitors, including p57$^{Kip2}$ and p21$^{Cip1}$, and upregulated the expression of these genes in mRNA and protein levels. And we also showed that loss of Znhit1 lead to lens fibrosis by upregulating the expression of p21$^{Cip1}$.

**Conclusions.** Our findings suggested that Znhit1 is required for the survival of lens epithelial cells. The loss of Znhit1 leads to the overexpression of p21$^{Cip1}$, further resulting in lens fibrosis, and impacted the establishment of lens transparency.

Keywords: zinc finger HIT-type containing 1 (Znhit1), p21$^{Cip1}$, lens, fibrosis, cataract

The ocular lens is a transparent and avascular tissue located in the eye behind the iris, and the main function is to efficiently refract light onto the retina for near and far visual targets. The lens is composed of two morphologically different cell types: a monolayer of cuboidal lens epithelial cells lines the inner surface of the anterior lens capsule and elongated lens fiber cells that are located at the posterior pole form the bulk of the lens tissue. During lens development, lens progenitor cells proliferate and migrate to the equator, where they exit the cell cycle and convert to lens fiber cells.[1–4] During terminal differentiation, the fiber cells form in a precisely aligned hexagonal arrangement and express abundant crystallin proteins. The highly ordered alignment of the differentiated cells minimizes the scattering of light that enters through the pupil.[3] Defects that occur during the development of the mature lens fiber cells lead to cataract formation.[5] Although several signaling pathways and some effectors have been defined for lens development, the epigenetic regulation of lens embryogenesis remains to be determined.[6,7]

Chromatin remodeling is a key step in the epigenetic regulation of gene transcription in eukaryotes.[8,9] During embryogenesis, ATP-dependent chromatin remodeling complexes such as SWI/SNF, ISWI, CHD, and INO80 control chromatin accessibility to regulate cell fate determination.[10,11] The SRCAP complex belongs to the INO80 family and its core components contains catalytical subunit SRCAP (3230 amino acids, molecular weight 334 kDa) and other much smaller subunits zinc finger HIT-type containing 1 (Znhit1) or p18$^{Hamlet}$ (154 amino acids, molecular weight

17.5 kDa), YL-1, and ARP6. At the molecular level, this complex can replace histone H2A with its variant H2A.Z in the nucleosomes to regulate chromatin remodeling and gene transcription.[12–17] Znhit1 as a core subunit of the SRCAP complex has been proved to exert crucial function in maintaining the role of the complex.[14,18–21] During mammalian organ development and tissue homeostasis, Znhit1 controls intestinal stem cell maintenance and preserves hematopoietic stem cell quiescence.[20,21] However, how Znhit1 regulates lens development is completely unknown.

In this study, we constructed a lens-specific Znhit1 conditional knockout (Znhit1 cKO) mouse strain to investigate the biological functions of Znhit1 in lens development. The Znhit1 cKO mice had a severe cataract and microphthalmia phenotype. The depletion of Znhit1 increased the expression of $p57^{Kip2}$ and $p21^{Cip1}$ in mRNA and protein levels, which caused cell cycle arrest. In Znhit1 cKO mice, the loss of Znhit1 caused lens fibrosis, which is regulated by the overexpressed $p21^{Cip1}$. And in vitro experiments provided compelling evidence that Znhit1 regulates the expression of $p21^{Cip1}$ to exert its function. Taken together, our findings establish the vital role of Znhit1 in cell cycle exit and lens transparency.

## Methods

### Animal Experiments

The use of animals in this research was approved by the Animal Care and Ethics Committee at Wenzhou Medical University, Wenzhou, China. All breeding and experimental procedures were conducted in accordance with the Association for Research in Vision and Ophthalmology statement.

*Znhit1*$^{fl/fl}$ mice were generated by Model Animal Research Center of Nanjing University (Nanjing, China).[20] The targeting strategy is shown in Supplementary Figure S1A. *Mlr10-cre* mice were obtained from Dr. Michael Robinson. *Mlr10-cre* mice were on a FVB background and backcrossed to wild-type C57BL/6J mice to generate cre-transgenic mice on the C57BL/6J background.[22] For the *Mlr10-cre* line, the expression of cre were restricted to the lens epithelial and fiber cells.[23] All mice were maintained in C57BL/6 background, and genotypes were determined by the relevant primers (Supplementary Figs. S1B, C, Supplementary Table S1). Pregnant mice were euthanized by $CO_2$ inhalation, and embryos were harvested for follow-up experiments. For subsequent experiments, postnatal mice were euthanized by anesthesia using a mixture of ketamine (96 mg/kg) and xylazine (14.4 mg/kg) via intraperitoneal injection.

UC2288 (ab146969, Abcam, Cambridge, UK) were dissolved in DMSO (D2650, Sigma-Aldrich, St. Louis, MO). For the following experiments, mice were randomly divided into two subgroups. Vehicle-treated mice, designated as Znhit1 cKO + DMSO, received only the solvent. UC2288 (10 mg/kg body weight) was administered by intraperitoneal injection four times per week, designated as Znhit1 cKO + UC2288.

### Preparation of Mouse Embryo Fibroblasts (MEFs) and siRNA Knockdown

We used C57BL/6 pregnant mice for MEFs isolation. Female mice on days 13 to 16 of gestation were euthanized and dissected to extract the fetuses. The heads and visceral tissues of the fetuses were discarded, and the remaining tissues were washed two times in cold Dulbecco's phosphate-buffered saline (14190144, Gibco, Carlsbad, CA). The washed tissues were then cut into tiny pieces and transferred into a 15-mL centrifuge tube. After centrifugation at 1500 × *g* for 5 min at 4°C, the tissue pieces were rinsed with 10 mL 0.05% trypsin for 30 min at 37°C. To fully digest the tissues, they were shaken gently every 5 min. Afterward, the digestion medium was neutralized with MEFs growth medium (DMEM [11995, Gibco] supplemented with 2 mM L-glutamine [35050061, Gibco], 100 U/mL of penicillin-streptomycin [15140122, Gibco], and 10% fetal bovine serum [10099141C, Gibco]). The suspended cells, tissue fragments, and debris were then filtered, centrifuged, and the cells were counted. We use trypan blue (C0011, Beyotime Biotechnology, Shanghai, China) to determine cell viability, and the living cells were seeded at $3 \times 10^6$ cells in 75 $cm^2$ culture flasks. After 24 h, the culture medium was changed.

The siRNAs against *Znhit1*, *p21* were designed by and purchased from Gene Pharma Co., Ltd. (Shanghai, China) and RiboBio Co., Ltd. (Guangzhou, China), and were transfected into the MEFs using Lipofectamine RNAiMAX Transfection Reagent (13778150, ThermoFisher Scientific, Waltham, MA). The negative control (NC), Znhit1, and p21 siRNA sequences were designed and synthesized as follows:

si-NC: 5′-UUCUCCGAACGUGUCACGUTT-3′/5′-ACGUGACACGUUCGGAGAATT-3′
si-Znhit1-Mus: 5′-GAGCAGAACCUGAGUGCAUTT-3′/5′-AUGCACUCAGGUUCUGCUCTT-3′
si-p21-Mus: 5′-CGAGAACGGTGGAACTTTG-3′

### Histology

For histology, the tissues were extracted and fixed in a mixture of formaldehyde:ethyl alcohol:dd$H_2O$:acetic acid glacial (1:4:4:1) at room temperature (RT) for 24 h. After alcohol dehydration, the tissues were embedded in paraffin. To clearly display the difference of section direction, schematics of lens cross-section and lens longitudinal section were shown in Figure 1A. Slices (5-µm thick) were then stained with hematoxylin and eosin. Masson staining was performed as instructions.

### Terminal Deoxynucleotidyl Transferase-Mediated dUTP Nick-End Labeling (TUNEL) Staining

TUNEL staining, which identifies apoptotic cells, was performed using the In Situ Cell Death Detection Kit (12156792910, Roche, Basel, Switzerland) on cryosections according to the manufacturer's instructions. Apoptosis rates were calculated as the ratio of TUNEL-positive cells to DAPI-positive cells in controls and Znhit1 cKO lenses, and results were analyzed by the Student *t*-test.

### Immunofluorescence and Confocal Microscopy

For immunofluorescence microscopy, the tissues were fixed in freshly prepared 1% paraformaldehyde for 5 h at 4°C. The tissues then were dehydrated in a gradient of sucrose solutions at 4°C, embedded in Tissue Tek O.C.T. Compound (4853, Sakura Finetek, Torrance, CA), frozen in liquid nitrogen, and stored at –80°C until sectioned (10-µm thick).

Investigative Ophthalmology & Visual Science

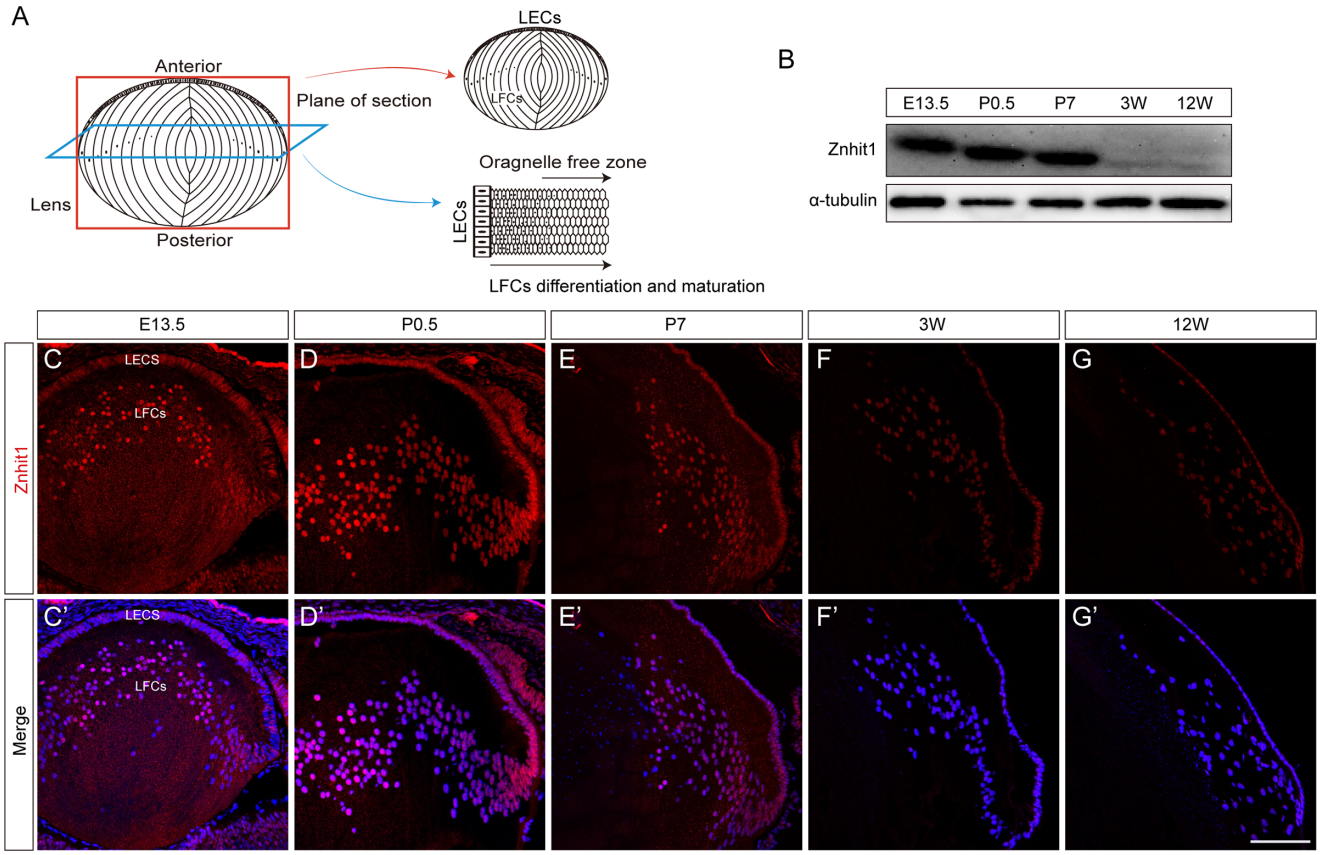


**Figure 1.** Expression of Znhit1 in lens. (**A**) Schematic of mice lens section. Diagram of a lens (*left*) with the longitudinal section plane (*red*) through the lens pole and the cross-section plane (*blue*) through the lens equator. Schematics (*right*) of the resulting lens longitudinal section (*up*) and lens equatorial cross-section (*down*). The longitudinal section of lens showed that lens fiber cells nuclei gradually move to the anterior and subsequently eliminate during lens maturation. And the cross-section of lens showed that epithelial cells are located at the periphery and hexagonal morphology of fiber cells are orderly arranged. (**B**) Expression pattern of Znhit1 during mouse lens development as shown by Western blot. $\alpha$-Tubulin served as the loading control. (**C–G′**) Distribution of Znhit1 proteins (*red*) during normal C57BL/6 mouse lens development was assessed by immunofluorescence microscopy. Znhit1 puncta were located in the lens epithelial and fiber cells. LECs, lens epithelial cells; LFCs, lens fiber cells. Merge, combined immunolabeled and DAPI-stained images. Scales bars, 100 µm.

After rinsing, the frozen slices were immersed in blocking buffer (4% bovine serum albumin, 0.5% Triton X-100 in 0.1 M PBS) for 2 h at RT. The slices were then incubated with primary antibodies overnight (≥16 h) at 4°C. Staining was achieved by the appropriate secondary antibodies. A full list of antibodies is shown in Supplementary Table S2. Images were collected using a Zeiss LSM880 with Airyscan confocal microscopy (Zeiss, Göttingen, Germany).

The proliferation rates in the lens epithelium were calculated as the ratios of Ki67-positive cells to DAPI-positive cells within the epithelium and the statistical significances between controls and Znhit1 cKO lenses were evaluated by the Student *t*-test.

## Western Blot Analysis

Lenses and MEF cells were homogenized in icy radio immunoprecipitation assay lysis buffer (P0013B, Beyotime Biotechnology) with 1 mmol/L phenylmethylsulfonyl fluoride (ST506, Beyotime Biotechnology) and Complete Protease Inhibitor Cocktail (11836153001, Roche). The proteins were separated on a 12% sodium dodecyl sulfate-polyacrylamide gel, and then transferred to a polyvinylidene fluoride membrane (IPFL00010, Millipore, Billerica, MA). Membranes were blocked using nonfat milk (dissolve in TRIS-buffered saline containing 0.1% Tween 20 [A600560-0500, Sangon Biotech, Shanghai, China]) for 1.5 h at RT and incubated with primary antibody overnight at 4°C. They were then incubated with secondary antibodies for 2 h at RT. The information of antibodies is shown in Supplementary Table S2.

Densitometric analysis of the protein bands was conducted using Image J software (National Institutes of Health, Bethesda, MD), and the values were normalized to the corresponding loading control, glyceraldehyde phosphate dehydrogenase (GAPDH) or $\alpha$-Tubulin. For each experiment, at least three extracts from control and Znhit1 cKO tissues were analyzed.

## RNA Extraction, cDNA Preparation, and Quantitative RT-PCR

Total lens RNA was extracted using the RNeasy Fibrous Tissue Mini Kit (74704, Qiagen, Valencia, CA) according to the manufacturer's instructions. Then the lens RNA was treated with RQ1 RNase Free DNase (M6101, Promega, Madison, WI) to inactivate DNA. The cDNAs were

Investigative Ophthalmology & Visual Science

synthesized using random primers (C1181, Promega) and Moloney Murine Leukemia Virus Reverse Transcriptase (M1701, Promega). quantitative RT-PCR was performed with the specific primers (Supplementary Table S1) and Power SYBR Green PCR Master Mix (4367659, Applied Biosystems, Carlsbad, CA) on an Applied Biosystems ViiA 7 Real-Time PCR system. The expression of mRNA relative to GAPDH was determined by using threshold cycle values and the $^{\Delta\Delta}$Ct method.[24]

### RNA Sequencing (RNA-seq)

The collection of lenses from P0.5 eyes and total RNA extraction was as described elsewhere in this article. Three biological replicates of RNAs from different *Znhit1*$^{Mlr10\text{-}cre}$ and *Znhit1*$^{Ctrl}$ mice were used. High-throughput sequencing was performed using an Illumina Novaseq platform (San Diego, CA). For each sample, the RNA-seq data was mapped by Hisat2 with no more than two mismatches to the reference genome, and then only the uniquely mapped reads were used to estimate the gene level expression values by fragments per kilobase of exon model per million mapped fragments.[25,26] The statistical significance tests of differentially expressed genes were performed by DEseq2R package.[27] Corrected *P* values of 0.05 and absolute foldchanges of 2 were set as the threshold for significantly differential expression. Enrichment analysis of differentially expressed genes was implemented by the cluster Profiler R package.[28]

### Assay for Transposase Accessible Chromatin Using Sequencing (ATAC-seq)

ATAC-seq of Znhit1 cKO and control lenses were performed by Romics (Shanghai, China). We collected frozen lens samples of control and Znhit1 cKO at P0.5, each sample extracted more than 40,000 nuclei for following steps. Two biological replicates from different *Znhit1*$^{Mlr10\text{-}cre}$ and *Znhit1*$^{Ctrl}$ mice were used. Quality filtered reads were then mapped to the GRCm38/mm10 reference genome using the Burrows–Wheeler Aligner program, and MASC2 software for peak calling with a *q*-value of less than 0.05 set as the cut-off.[29,30] The HOMER's findMotifsGenome.pl tool was used for motif analysis. Differentially accessible regions (DARs) were annotated by the function of HOMER's annotatePeaks.pl.[31]

### Statistical Analysis

All data were analyzed by GraphPad Prism 8 (GraphPad Inc., La Jolla, CA) and expressed as the means ± standard deviation. Data analysis was performed on a minimum of three mice for each genotype. For comparison of two groups, the differences were assessed by Student *t*-test. One-way ANOVA was performed for comparisons among more than two groups. *P* values of less than 0.05 were considered significant and noted with asterisks.

## Results

### Ablation of Znhit1 Causes Lens Defects

The SRCAP complex is one of the ATP-dependent chromatin remodeling complexes and can replace histone H2A with its variant H2A.Z in nucleosomes for activation of gene transcription.[17] Gene transcription is of crucial importance during lens development, playing complex and extensive roles in cell fate decisions and tissue morphogenesis.[32,33] Znhit1 is a core subunit of this complex; we speculate that Znhit1 could regulate gene expression and play essential roles during lens development.

To analyze the molecular function of Znhit1 during lens development, we first determined the expression pattern of the Znhit1 protein. By immunofluorescence microscopy and Western blot analysis, we observed that the expression of lens Znhit1 in wild-type mice stayed at a high level throughout the embryonic (E13.5) and early postnatal (P0.5 and P7) stages. However, expression gradually diminished during the growth to adulthood (Figs. 1B–G′). The strong expression pattern in the early stages of lens development suggested that Znhit1 may have special roles in mouse lens morphogenesis.

To understand the roles of Znhit1 in mouse lens growth, we deleted Znhit1 using the *Mlr10-cre* transgene crossed with *Znhit1*$^{fl/fl}$ mice. The lenses of newborn *Znhit1*$^{fl/fl}$*; Mlr10-Cre*$^{+}$ mice (referred to as Znhit1 cKO) exhibited serious lens differentiation defects (described elsewhere in this article). And, the *Znhit1*$^{fl/fl}$*; Mlr10-Cre*$^{-}$ littermates were normal and served as controls. For Mlr10 mice, cre expression was started at E10.5, and detectable in the majority of both the lens epithelium and differentiating lens fiber cells at E12.5.[23] By immunofluorescence microscopy, we found that the expression of Znhit1 was decreased in both the lens epithelial cells and fiber cells of Znhit1 cKO at E13.5 and newborn of P0.5 (Figs. 2A–D′). Further examination of Znhit1 mRNA and protein levels confirmed the Znhit1 deletion in mouse lens cells at P0.5 (Figs. 2E–G).

In 3-week-old mice, approximately 61% of the Znhit1 cKO mice had a severe cataract phenotype compared with control groups (Figs. 3A–B′). The 12-week-old control mice had normal sized eyes with lenses that were transparent and smooth. In contrast, the 12-week-old Znhit1 cKO mice had microphthalmia, and the lenses were small, hard, opaque, and lacked a regular and smooth surface (Figs. 3C, D), implying a lack of transparency, which were similar to lens fibrosis phenotype. Microphthalmia suggested reduced cell growth and/or increased cell apoptosis in the anterior cells of the lens vesicle due to the deletion of Znhit1. Consistent with the phenotype, deletion of Znhit1 increased programmed cell death, as revealed by TUNEL staining (Figs. 4A–B″). In contrast, we estimated cell proliferation by analysis of the expression of the Ki67 protein (Figs. 4C–D″), a marker specifically expressed in proliferating cells that are not in $G_0$.[34] Collectively, these data likely accounted for the smaller size in Znhit1 cKO lenses.

### Loss of Znhit1 Disrupts Lens Differentiation

Next, we performed a histological assessment to investigate the morphological alterations in Znhit1 cKO lenses at different stages. At E13.5, lenses underwent primary lens fiber cell differentiation that fill the lumen of the lens vesicle.[6] The lens structures appeared to be normal in both the control and Znhit1 cKO eyes at E13.5 (Figs. 5A, A′). At E15.5, the primary lens fiber cells of the control lenses reached the lens epithelium, and the lens epithelial cells located at the equator were differentiating into secondary fiber cells (Figs. 5B, 5C). However, the Znhit1 cKO lenses at E15.5 had accumulations of nucleated cells at the lens posterior pole (Figs. 5B′, 5C′). And at E17.5, the growth deficiency of Znhit1 cKO lens was similar with E15.5 (Figs. 5D–D′). At

Investigative Ophthalmology & Visual Science

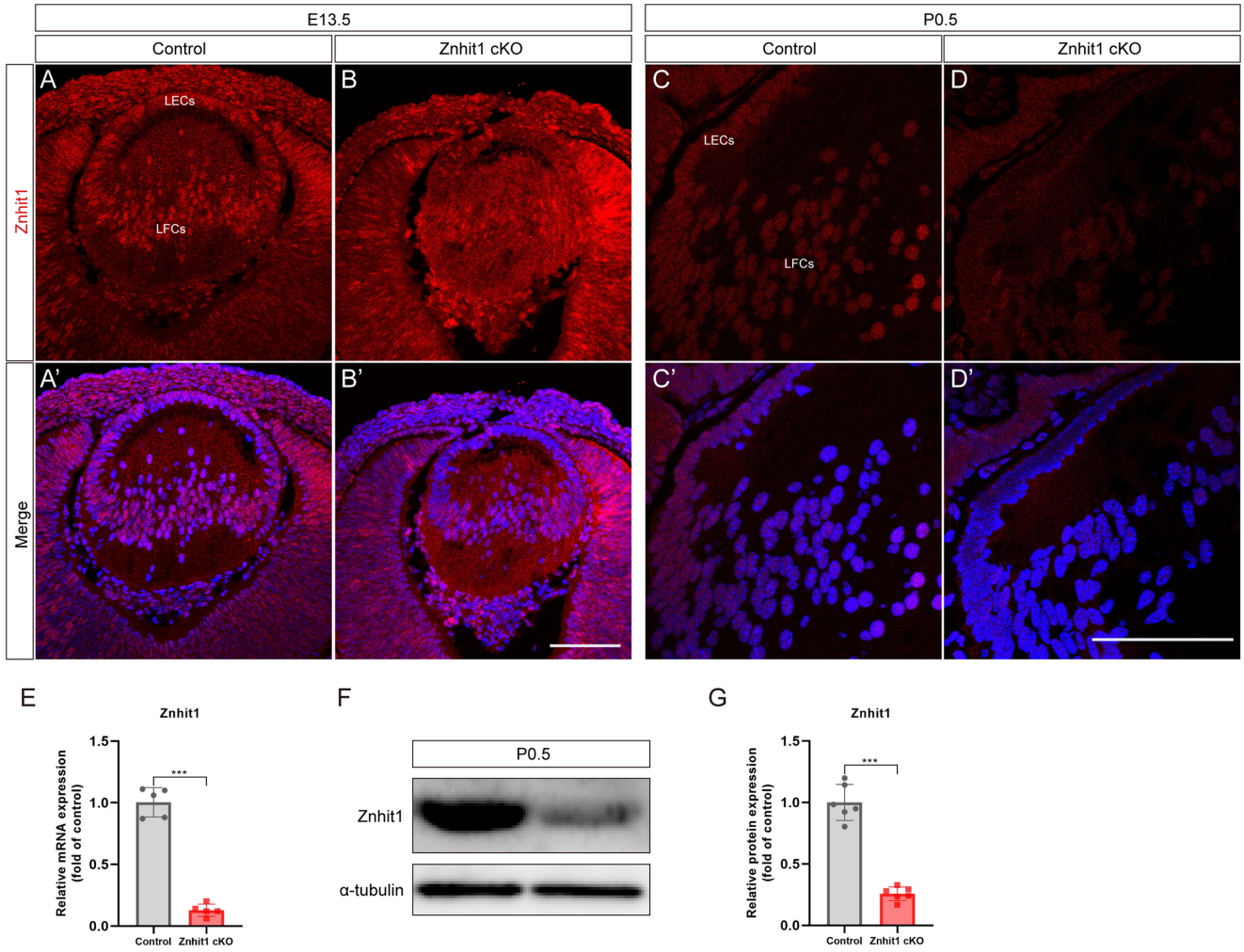


**Figure 2.** Tissue-specific Znhit1 deletion in lens. (**A–D′**) Immunofluorescence analysis of Znhit1 expression (*red*) in E13.5 and P0.5 control and Znhit1 cKO lenses. (**E**) Lenses were harvested from control and Znhit1 cKO mice at P0.5 to examine Znhit1 mRNA expression by quantitative RT-PCR. GAPDH was used as the internal control. (**F, G**) Lenses were isolated from control and Znhit1 cKO mice at P0.5 for western blot examination of Znhit1 expression. α-Tubulin served as the loading control. All values were expressed as means ± standard deviations. Merge, combined immunolabeled and DAPI-stained images. Scales bars, 100 µm. Student *t*-test: $^{***}P < 0.001$.

postnatal stages P0.5 and P7, the Znhit1 cKO lens fiber cell nuclei had moved to the posterior pole, and there was progressive deterioration in which the lens fiber cell region had numerous vacuoles (Figs. 5E–H′), indicating severe defects of lens development. In transverse sections of control mice lenses at P7, the hexagonal fiber cells had a highly ordered arrangement (Figs. 5I). However, the lens fiber cells of the Znhit1 cKO mice were formed into irregular cellular structures and vacuoles (Figs. 5I′).

Using phalloidin staining for F-actin showed that control lenses exhibit normal cellular patterns (Supplementary Figs. S2A–A′). In contrast, deletion of Znhit1 caused disordered and abnormal fiber cells organization and morphology (Supplementary Figs. S2B–B′). During lens development, the transcription factors Pax6 and Prox1 critically regulate the normal differentiation of the transparent lens. Pax6 controls lens induction and fate determination while Prox1 regulates fiber cells elongation, differentiation and morphogenesis.[35,36] Interestingly, albeit the severe morphological defects including the numerous vacuoles and accumulations of nucleated cells at the lens posterior pole, Pax6 and Prox1 were still expressed in Znhit1 cKO lenses (Supplementary Figs. S2C–F′). In addition, the polarity of the lens fiber cells was also preserved as evidenced by the location of N-cadherin (Supplementary Figs. S2G–H′), respectively.

Taken together, these data indicated that Znhit1 proteins are dispensable for lens fiber cells elongation and polarity, but are essential for proliferation, survival of the epithelial cells, and organization of the fiber cells that make up the structurally transparent lens.

## Loss of Znhit1 Leads to Lens Fibrosis

Based on the morphological alterations, such as disorganization of lens fiber cell morphology and stiff tissue architecture, we hypothesized that Znhit1 inactivation activates the expression of myofibroblasts, which can lead to progressive fibrosis. Indeed, Znhit1 knockout induces the expression of myofibroblasts marker α-smooth muscle actin (α-SMA),[37] focal adhesion protein vinculin, as well as extensive accumulation of extracellular matrix, including expression of fibronectin, gradually increased from P0.5 to P14 of Znhit1

Investigative Ophthalmology & Visual Science

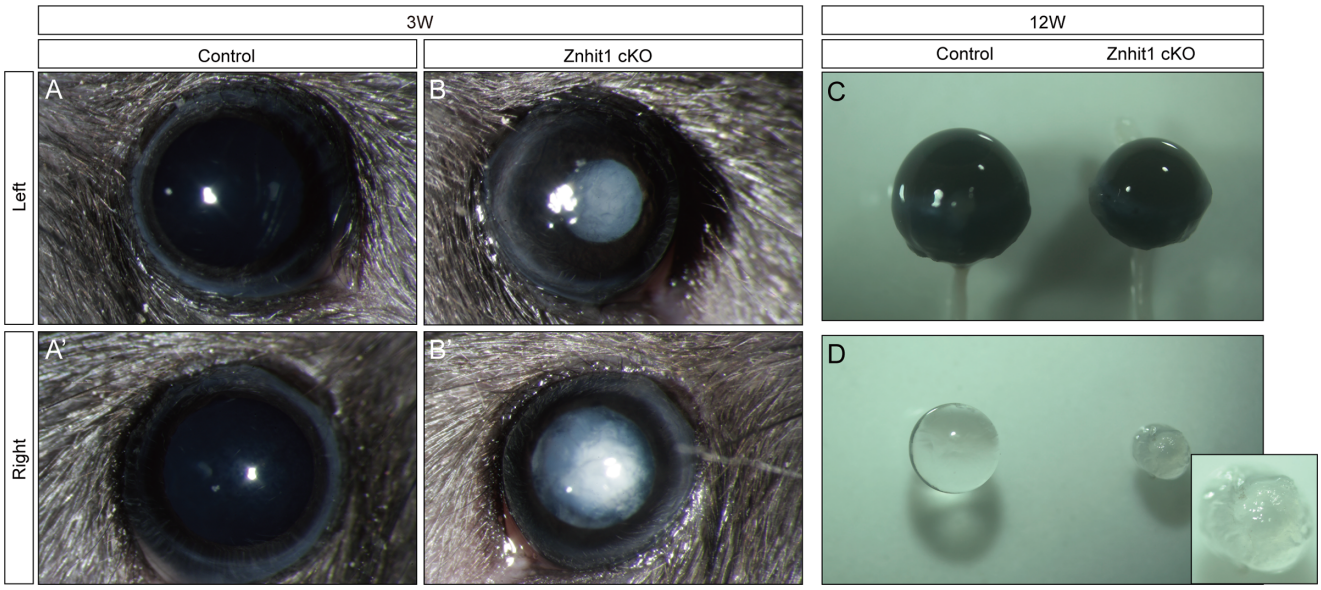


**Figure 3.** Cataract and microphthalmia phenotype in Znhit1 cKO mice. (**A, B′**) Slit lamp view of a 3-week-old mice lens showing the cataract phenotype in Znhit1 cKO. (**C, D**) Representative images of eyes and lenses from control and Znhit1 cKO mice at 12 weeks. Znhit1 cKO mice had obvious microphthalmia and rough lenses. Inset image is magnified picture of Znhit1 cKO lens.

cKO mice (Fig. 6A, B). And Masson staining also showed Znhit1 cKO lens fiber cells were surrounded by extracellular matrix accumulation, compared with controls (Figs. 6C–F). These results revealed that Znhit1 deletion leads to lens fibrosis lesions, likely causing organ deformation and dysfunction. To figure out the molecular mechanisms of cKO Znhit1–caused fibrosis, we further performed in vivo and in vitro experiments.

## Znhit1 Deletion Increases Chromatin Accessibility of CDKIs

The INO80 chromatin remodeling complexes regulate gene expression through specific molecular mechanisms.[38] Thus, we performed RNA-seq to analyze Znhit1-regulated genes. We found 1766 differentially expressed transcripts in the Znhit1 cKO lenses, including 958 upregulated and 808 downregulated genes (fold change $> 1.0$; $P < 0.05$) (Fig. 7A). Gene ontology and Kyoto Encyclopedia of Genes and Genomes analyses showed that upregulated genes were involved in cell locomotion, cell migration, focal adhesion, and cell cycle (Supplementary Fig. S3A, B).

The INO80 chromatin remodeling complex modifies chromatin in many ways, including nucleosome sliding and replacement of variant histones that modulate chromatin accessibility and, consequently, regulate gene expression.[39,40] To determine whether Znhit1-mediated chromatin remodeling alters the organization of accessible chromatin, we performed ATAC-seq in control and Znhit1 cKO lenses. By analyzing the ATAC-seq data from two biological replicates, we found that Znhit1 deletion led to 14,586 changes in chromatin accessibility, including 6639 upregulated DARs and 7947 downregulated peaks (Fig. 7B). The opened ATAC DARs were present mainly in the promoters, where most transcription factor binding sites are located.[41] The closed ATAC DARs were accumulated in intergenic regions and introns, indicating that Znhit1 in mouse lenses mainly regulates the accessibility of chromatin. The altered ATAC DARs were annotated to a total of 5654 genes. Comparing them with the Znhit1-regulated genes identified by RNA-seq, we found that 312 Znhit1-regulated genes had significant changes in chromatin accessibility (Fig. 7C). Several cell cycle regulators have been examined that are particularly significant for maintaining normal patterns of lens cell proliferation, including CDKIs and fibroblast growth factor signaling.[7] And the data showed that Znhit1 deletion led to increased accessibility of promoter regions of cyclin-dependent kinase inhibitors, $p57^{Kip2}$ (Cdkn1a) and $p21^{Cip1}$ (Cdkn1c), all of which function mainly in cell cycle regulation (Fig. 7D). However, loss of Znhit1 did not change the chromatin accessibility of $p27^{Kip1}$ (Cdkn1b), another member of the cyclin-dependent kinases inhibitors (Fig. 7D). Together, our results indicated that Znhit1 loss led to marked changes the in chromatin dynamics of the mouse lens.

Motif enrichment assays identified five of the most enriched transcriptional factor motifs in the differential chromatin-accessible regions of Znhit1 cKO lenses, including CTCF, CTCFL, SP1, SP2, and SP5 (Fig. 7E). These transcription factors were mainly associated with cell proliferation, cell differentiation, cell apoptosis, and embryogenesis.[42–44] Of note, it has been reported that multiple signaling pathways are associated with Sp1 regulation of the $p21^{Cip1}$ promoter.[45] These results demonstrated that Znhit1-mediated chromatin remodeling regulates, at least in part, access of transcription factors for transcriptional regulation.

## Dysregulation of CDKIs in Znhit1 cKO Lens Fiber Cells

To investigate the causes of disrupted lens development and determine whether lens fibrosis is coupled with cell cycle arrest, we examined the expression of genes involved in the control of cell cycle exit. In P0.5 control (Figs. 8A–A′) and Znhit1 cKO (Figs. 8B–B′) lenses, CDKI $p27^{Kip1}$ was

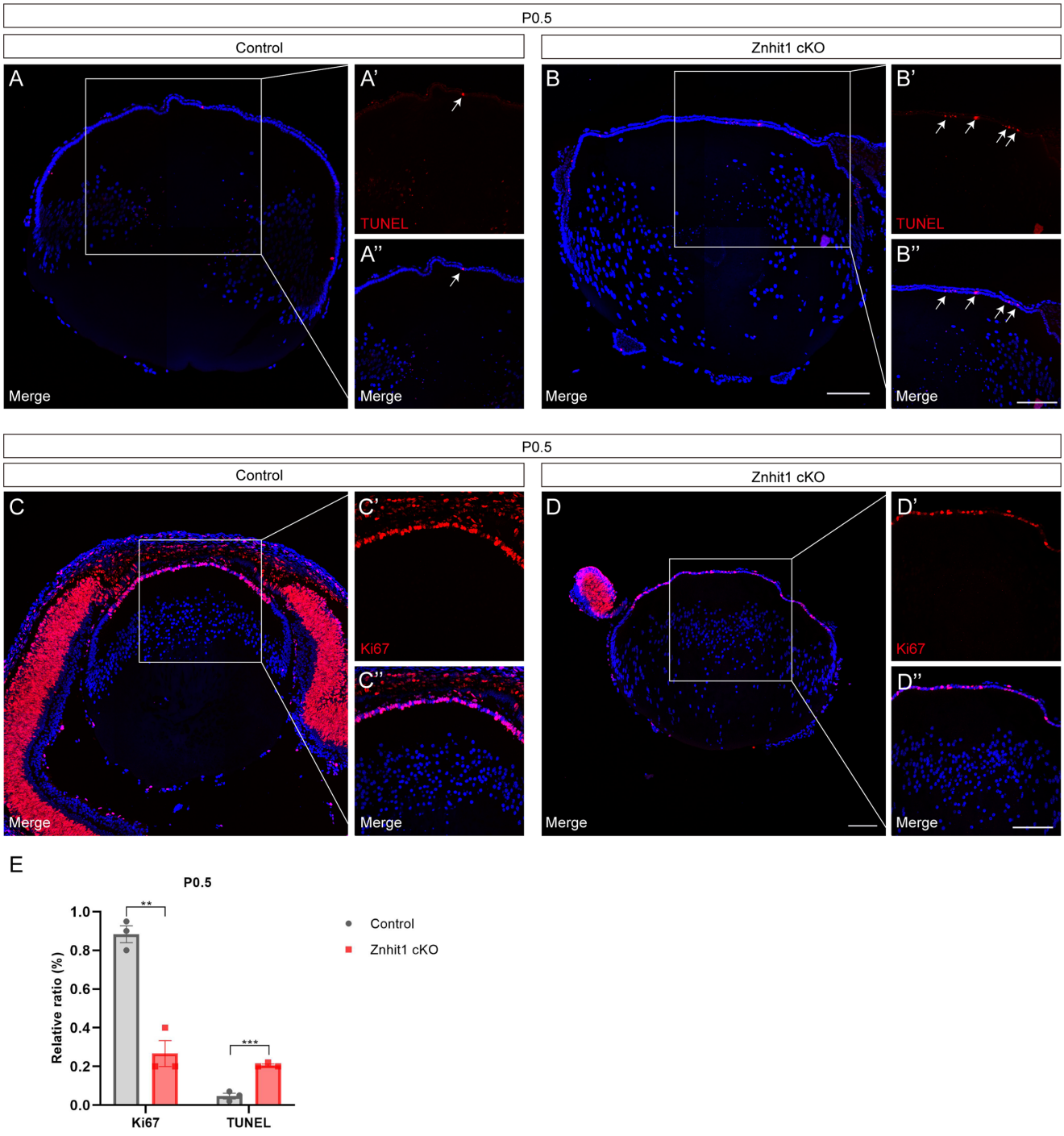


**Figure 4.** Depletion of Znhit1 decreased cell proliferation and increased cell apoptosis. (**A, B′′**) TUNEL staining (*red*) showed increased apoptotic epithelium (*white arrows*) in P0.5 Znhit1 cKO lenses. (**C, D′′**) Immunofluorescence staining of the proliferation marker Ki67 (*red*) in P0.5 control lenses showed that the proliferating epithelial cells were present from the anterior of the lens epithelium to the lens equator. In the Znhit1 cKO lenses, the number of proliferating lens cells was reduced. (**E**) Quantification of proliferation and apoptosis in control and Znhit1 cKO lenses. Merge, combined immunolabeled and DAPI-stained images. Scale bars, 100 µm. Student *t*-test: $^{**}P < 0.01$; $^{***}P < 0.001$.

similarly expressed in cells localized in the lens equatorial region that undergo cell cycle exit and are beginning to differentiate into lens fiber cells.[46] CDKI $p57^{Kip2}$ in control lenses were similarly distributed with $p27^{Kip1}$ (Figs. 8C–C′). However, in Znhit1 cKO lenses, the expression of $p57^{Kip2}$ was markedly elevated in the lens central region where cells had already exited the cell cycle and become differentiated (Figs. 8D–D′). Notably, quantitative RT-PCR (Supplementary Fig. S4) and Western blot analysis (Figs. 8E–F, 8J) indicated that, compared with controls, the expression of $p57^{Kip2}$ was increased and the expression of $p27^{Kip1}$ was unchanged in Znhit1 cKO lenses.

In normal lens development at P0.5, the expression of $p21^{Cip1}$ was not detected by immunofluorescence

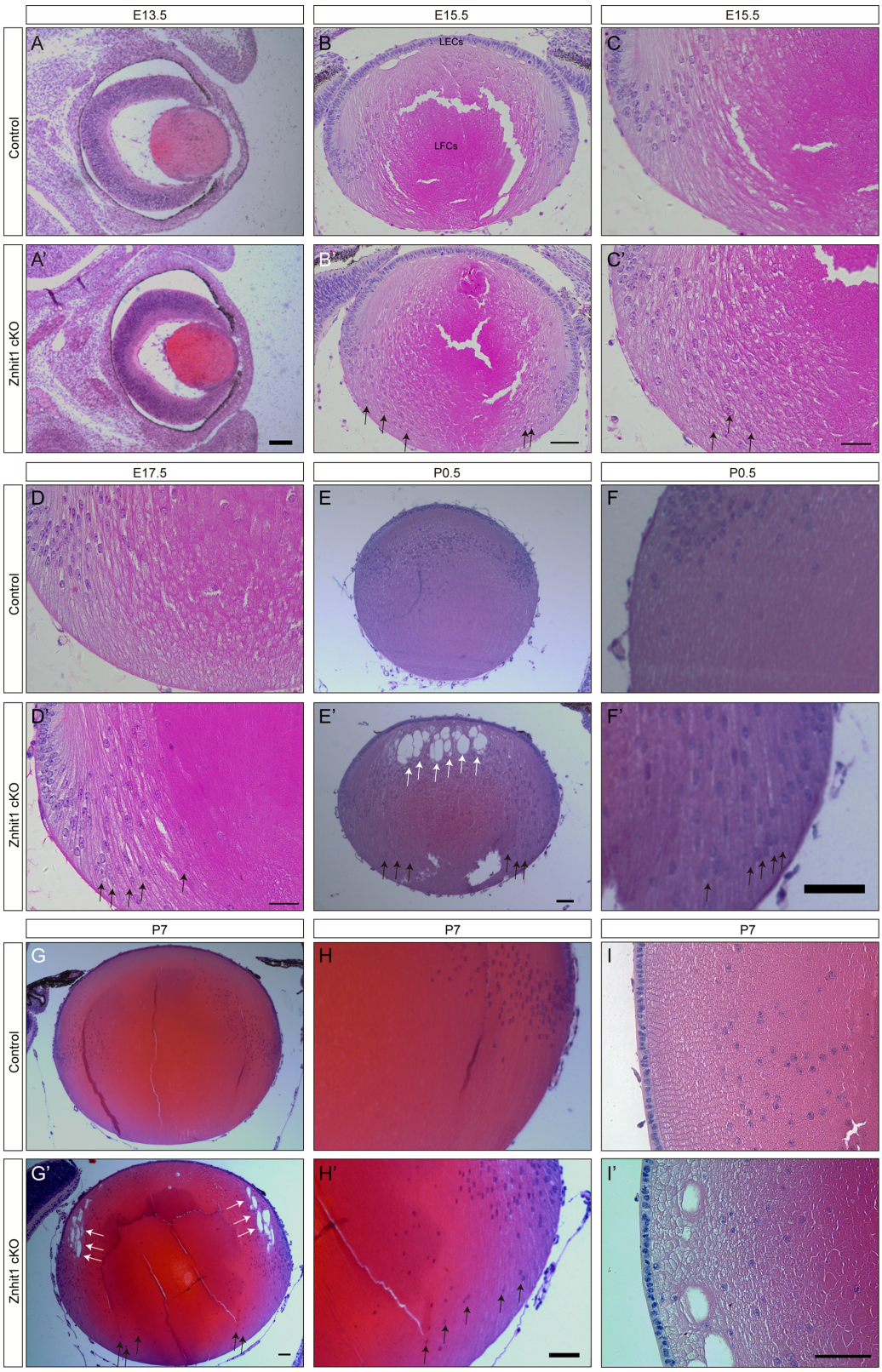


**Figure 5.** Znhit1 is necessary for mouse lens differentiation. (**A, A′**) Primary fiber cells fill the entire lens at E13.5. (**B–D′**) At E15.5 and E17.5, Znhit1 cKO lenses showed that fiber cell nuclei had moved to posterior pole (*black arrows*). (**E–H′**) The early stages (P0.5 and P7) of Znhit1 mutant lenses had numerous vacuoles in the fiber cell region (*white arrows*), as well as nuclei that were located at the posterior pole (*black arrows*). (**I, I′**) Compared with P7 controls, Znhit1 cKO lens fiber cells had an irregular and disorderly organization owing to the loss of hexagonal cellular structure. Scale bars, 50 µm.

Investigative Ophthalmology & Visual Science

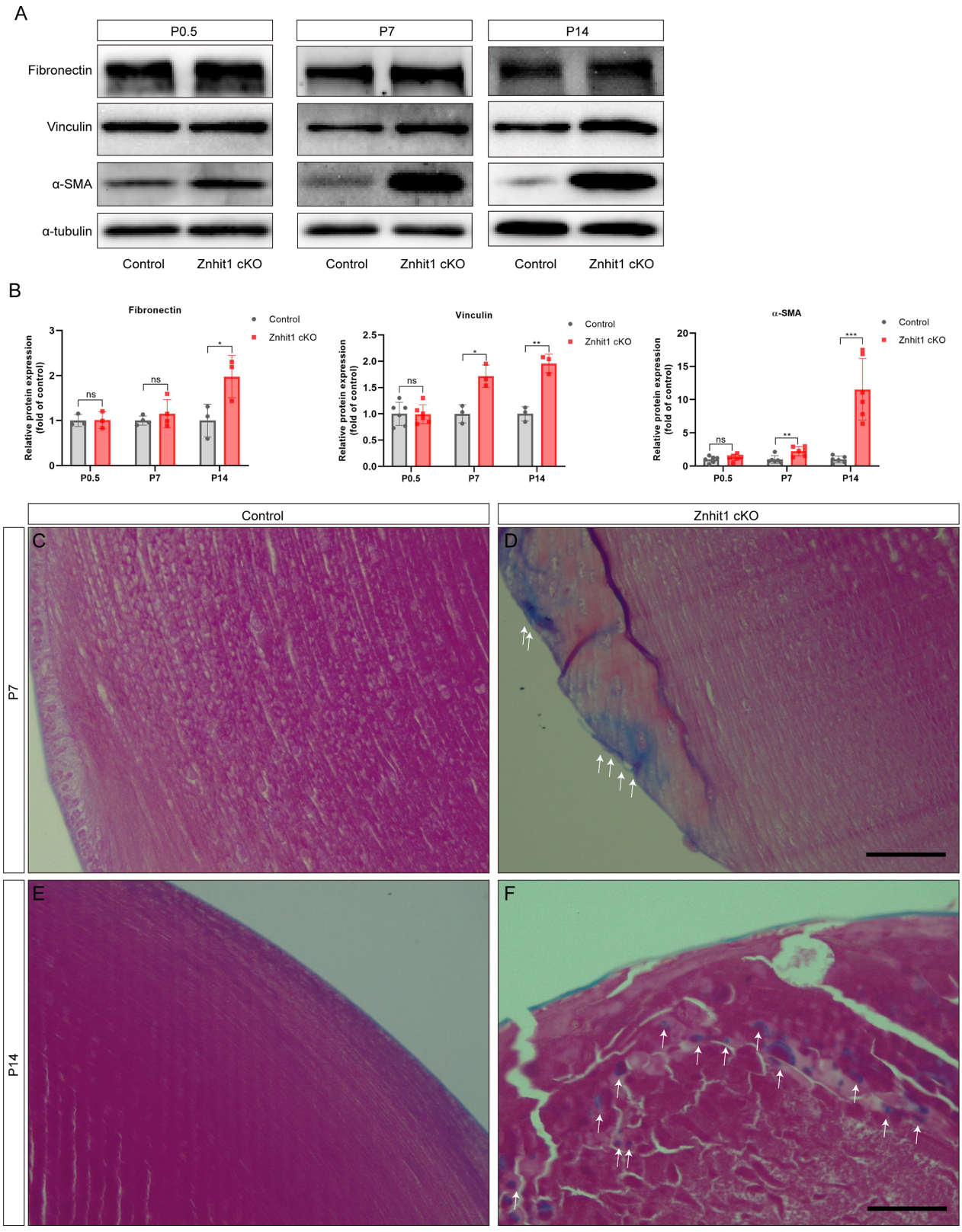


**Figure 6.** Loss of Znhit1 caused lens fibrosis. (**A**) At P0.5, P7, and P14, control and Znhit1 cKO lenses were isolated for Western blotting to examine the expression of fibronectin, vinculin and α-SMA. (**B**) Quantification of fibronectin, vinculin and α-SMA expression level in control and Znhit1 cKO lenses at P0.5, P7, and P14. α-Tubulin served as the loading control. (**C–F**) Masson staining showed increased extracellular matrix accumulation (*white arrows*) in P7 and P14 Znhit1 cKO lenses. All values were expressed as means ± standard deviations. Scale bars, 50 µm. Student *t*-test: $^{*}P < 0.05$; $^{**}P < 0.01$; $^{***}P < 0.001$.

Investigative Ophthalmology & Visual Science

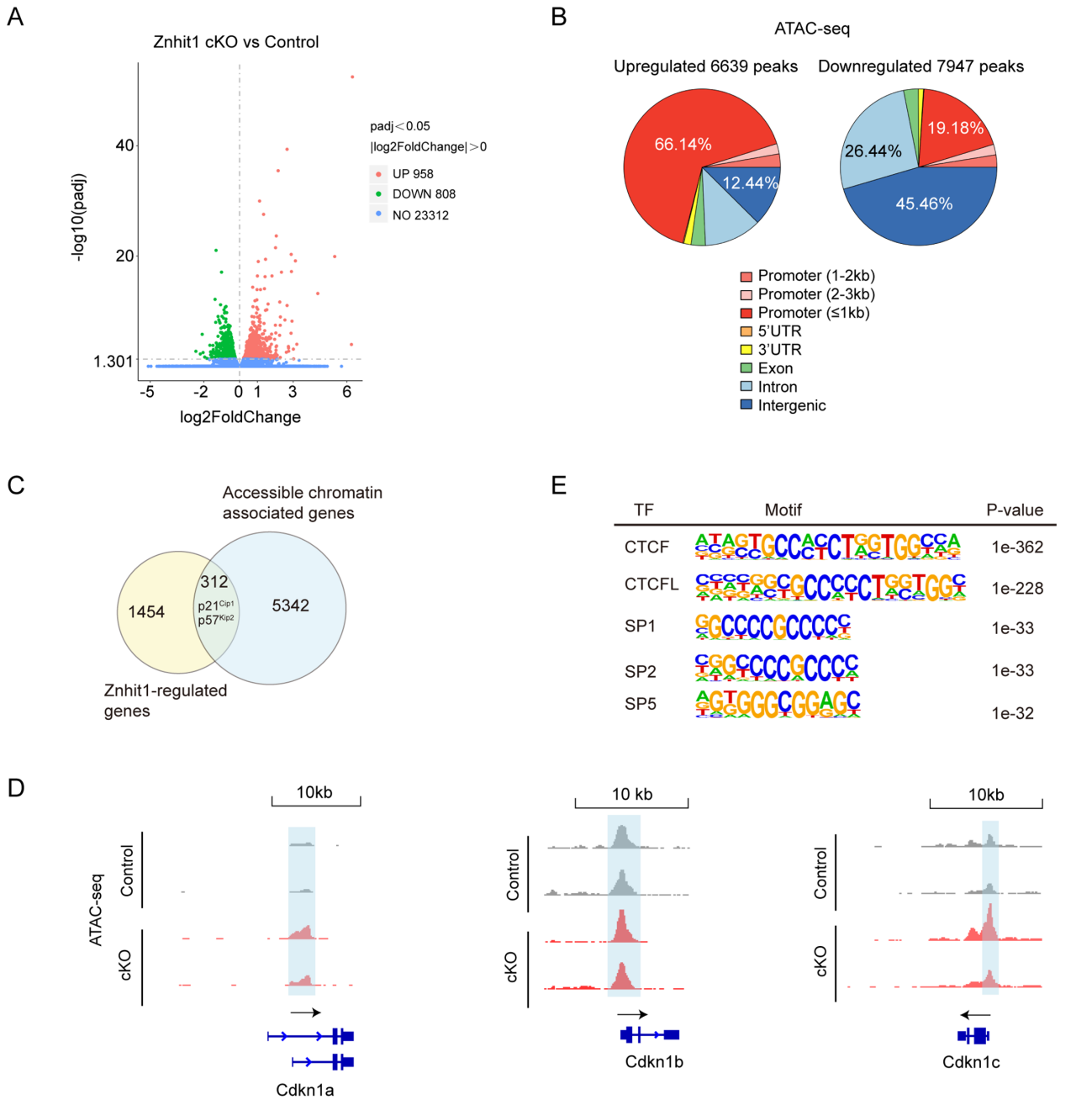


**Figure 7.** Deletion of Znhit1 alters the transcriptome in lens. (**A**) Volcano plot showed differentially expressed genes between Znhit1 cKO and control lenses at P0.5 ($n = 3$). *Red dots*, upregulated genes; *green dots*, downregulated genes. (**B**) Distribution of differentially accessible ATAC DARs in genome of control and Znhit1 cKO lenses. (**C**) Venn diagram indicating genes associated with the chromatin-accessible regions from ATAC-seq and differentially expressed genes from RNA-seq following Znhit1 knockout. (**D**) Changes in chromatin accessibility of Cdkn1a, Cdkn1b, and Cdkn1c genes. *Tracks in gray* show normalized and input-corrected ATAC-seq signal in control mice, and *tracks in red* show normalized and input-corrected ATAC-seq signal in Znhit1 cKO mice. The chromatin-accessible regions are indicated with *light blue bars* on the promoters. (**E**) Motif analysis of differential chromatin-accessible regions in Znhit1-regulated genes for putative transcription factor (TF)-binding sites by using HOMER database.

microscopy (Figs. 8G–G″), but in Znhit1 cKO mice at P0.5, it was ectopic expressed in differentiated lens fiber cells (Figs. 8H–H″). Moreover, the $p21^{Cip1}$ mRNA transcript levels were also increased in the Znhit1 cKO lenses (Supplementary Fig. S4). Western blot analysis also supported the upregulation of $p21^{Cip1}$ in Znhit1 cKO lenses (Figs. 8I–J).

Based on these results, the overexpression of CDKIs in Znhit1 cKO lens fiber cells indicated an aberrant differentiation process, especially at the terminal stages. Hence, the depletion of Znhit1 negatively regulated cell cycle progression, and sustained cell cycle arrest may result in maladaptive repair, eventually leading to tissue fibrosis.[47]

Investigative Ophthalmology & Visual Science

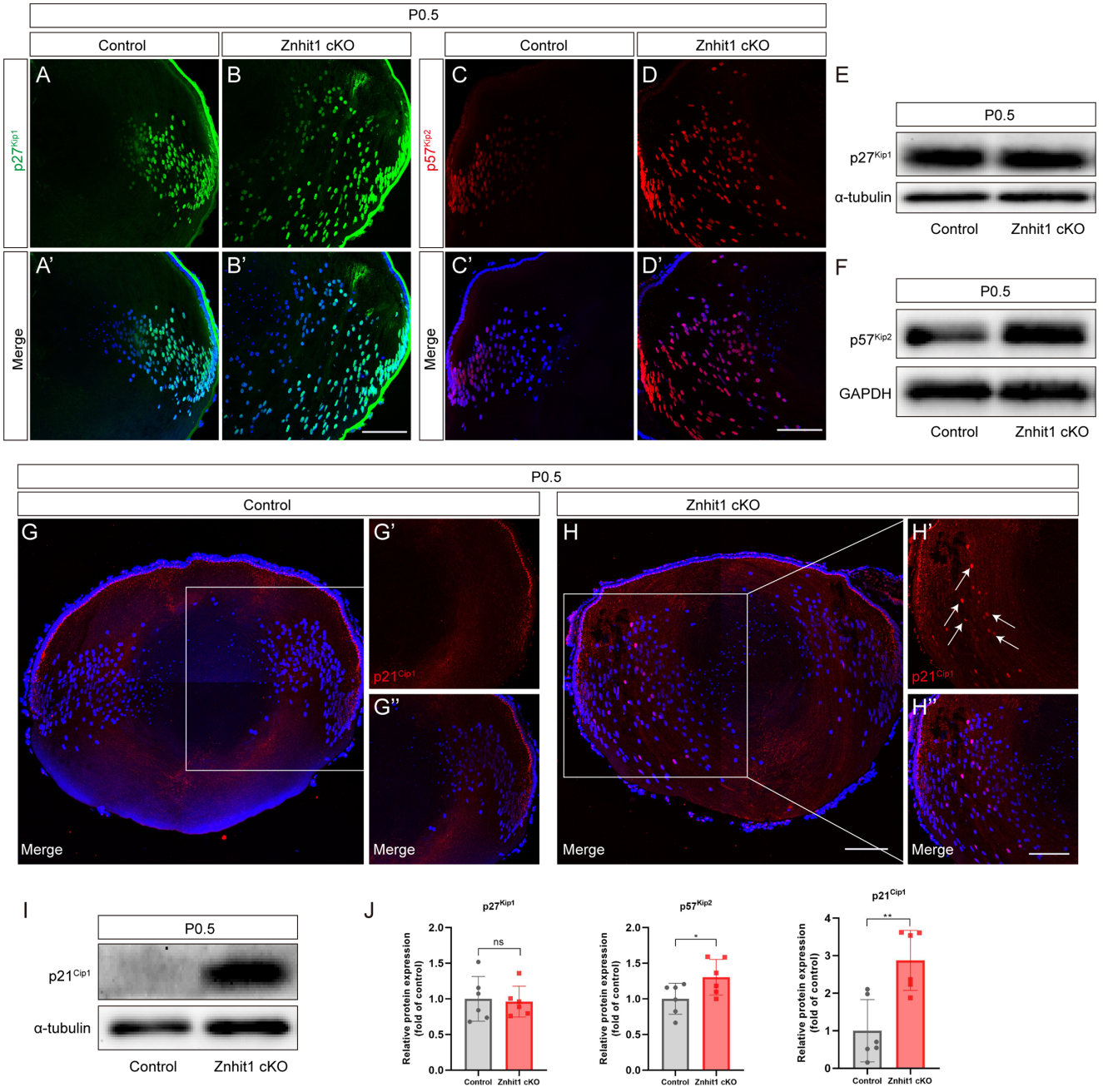


**Figure 8.** Depletion of Znhit1 disrupts expression of CDKIs in lens. (**A, B′**) At P0.5, in both control and Znhit1 cKO mice, $p27^{Kip1}$ (*green*) was expressed in lens fiber cells located at the lens equator transitional zone. (**C, D′**) At the same time, the distribution of $p57^{Kip2}$ (*red*) in Znhit1 cKO mice was greater in the central region of the lens compared to the controls. (**E, F**) Western blots of control and Znhit1 cKO lenses at P0.5 were examined for $p27^{Kip1}$ and $p57^{Kip2}$ expression. α-Tubulin/GAPDH served as the loading control. (**G–H′′**) The expression level of $p21^{Cip1}$, as shown by immunofluorescence microscopy, was repressed in the control mice at P0.5. In Znhit1 cKO mice, the expression of $p21^{Cip1}$ (*red*) in the nuclei (*white arrows*) was increased in the lens fiber cells. (**I**) Western blots of control and Znhit1 cKO lenses at P0.5 were examined for $p21^{Cip1}$ expression. α-Tubulin served as the loading control. (**J**) The protein relative expressions of $p27^{Kip1}$, $p57^{Kip2}$ and $p21^{Cip1}$ in control and Znhit1 cKO lenses were assessed by western blot. All values were expressed as means ± standard deviations. Merge, combined immunolabeled and DAPI-stained images. Scale bars, 100 µm. Student *t*-test: $^{*}P < 0.05$; $^{**}P < 0.01$.

## Upregulated $p21^{Cip1}$ in Znhit1 cKO Mice Caused Lens Fibrosis

Znhit1 cKO causes CDKIs overexpression that has a negative regulatory effect on cell cycle, as well as increases the proliferation of myofibroblasts, which leads to tissue contraction and dysfunction. Recent studies have suggested that the upregulation of the CDKI $p21^{Cip1}$ induces cell cycle arrest and mediates renal fibrosis and liver fibrosis.[48–50] Therefore, we considered the possibility that the upregulation of $p21^{Cip1}$ was associated with the fibrosis observed in the Znhit1 cKO lenses.

To further identify whether upregulated $p21^{Cip1}$ could have contributed to lens fibrosis, we used a recently

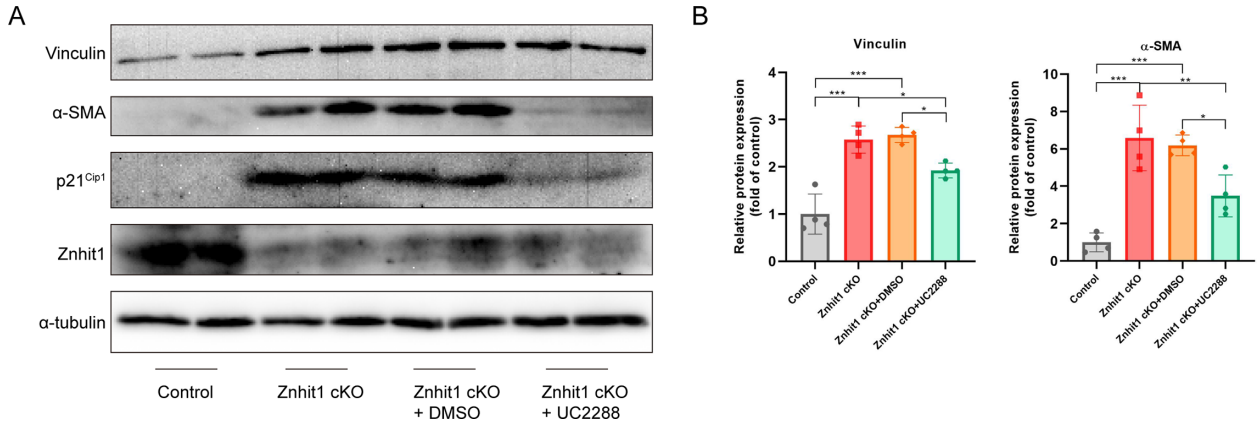


**Figure 9.** Upregulated p21$^{Cip1}$ caused lens fibrosis in Znhit1 cKO mice. (**A**) At P7, control, Znhit1 cKO, Znhit1 cKO + DMSO and Znhit1 + UC2288 lenses were isolated for western blotting to examine the expression of vinculin, α-SMA, p21$^{Cip1}$ and Znhit1. (**B**) Quantification of vinculin and α-SMA expression level in control, Znhit1 cKO, Znhit1 cKO + DMSO and Znhit1 + UC2288 lenses at P7. α-Tubulin served as the loading control. Student *t*-test: $^{*}P < 0.05$; $^{**}P < 0.01$; $^{***}P < 0.001$.

identified pharmacological p21$^{Cip1}$ inhibitor, UC2288, that downregulates p21$^{Cip1}$ levels through transcriptional and post-transcriptional mechanisms.[51] Then by treatment with UC2288, DMSO in Znhit1 cKO mice, we observed that treatment with UC2288 led to decreased p21$^{Cip1}$ levels. And compared with the Znhit1 cKO and Znhit1 cKO + DMSO groups, Znhit1 deletion combined with p21$^{Cip1}$ inhibition suppressed the expression of α-SMA and vinculin (Figs. 9A, B). These results provided compelling evidence that Znhit1 deletion caused p21$^{Cip1}$ overexpression, which further lead to myofibroblasts activation and lens fibrosis.

### Znhit1 Knockdown Causes Myofibroblasts Activation in MEFs

To further verify that Znhit1 could regulate p21$^{Cip1}$ to exert its function, we used primary MEF cells to explored the function of Znhit1 in vitro. We isolated MEFs from C57BL/6 embryos and infected them with siRNA to ablate Znhit1. We observed that si-Znhit1 in MEFs upregulated the expression of α-SMA and fibronectin (Figs. 10A, B). In conclusion, it seems that the knockdown of Znhit1 caused myofibroblast activation in MEFs.

To determine whether p21$^{Cip1}$ played a key role in the development of MEFs transdifferentiation, we were interested in the effects of knocking down Znhit1 individually or together with p21$^{Cip1}$ in MEFs. Surprisingly, the combined knockdown of Znhit1 and p21$^{Cip1}$ (si-Znhit1+p21$^{Cip1}$) in MEF cells rescued the si-Znhit1–induced fiber cells transdifferentiated into myofibroblasts, as detected by the decreased expression of α-SMA and fibronectin (Figs. 10A, B). Consistent with these results, immunofluorescence staining showed si-Znhit1 increased the expression of p21$^{Cip1}$ and α-SMA, and si-Znhit1+p21$^{Cip1}$ could rescue them (Figs. 10C–K′). Together, these results of in vitro experiments provide positive evidence that the loss of Znhit1 upregulated the expression of p21$^{Cip1}$, which further led to myofibroblast activation.

## Discussion

The ocular lens undergoes an orderly set of successive differentiation changes, including the regular arrangement of hexagonal fiber cells, accumulation of functional crystallin proteins, and degradation of subcellular organelles. The impairment of any of these processes leads to cataract formation, which is the leading cause of blindness. During embryogenesis, modifications of chromatin architectures allow the transcriptional activation or repression of particular genes. However, the molecular mechanisms of chromatin remodeling in lens development remain uncertain. Here, we examined the role of Znhit1 in mice lens embryogenesis and demonstrated that it is essential for lens fiber cell differentiation and lens transparency maintenance.

During lens development in mice, many signals are associated with lens placode invagination and lens vesicle formation.[6] Cells at the posterior lens vesicle differentiate into highly elongated primary lens fiber cells that fill the lumen of the lens vesicle at E13.5.[6] Soon thereafter, epithelial cells having a high proliferative index relocated to the germinative zone at a region anterior to the lens equator, where they differentiate into secondary lens fiber cells.[6,52] In histological analyses, we did not detect any morphological abnormalities in Znhit1 cKO lenses at E13.5. We speculate that, because *Mlr10-cre* is expressed from E10.5 and then expands to most of the lens cells by E12.5,[23] the duration of Znhit1 knockout may insufficient at E13.5 to impact the differentiation of lens fiber cells.

The balance between cell proliferation and differentiation requires the coordinated regulation of cell division cycle progression.[7] Changes in cell cycle states affect the determination of cell fate because cells in different cell cycle states have distinct molecular features and functions.[53] During the course of normal lens embryogenesis, the epithelial cells at the lens equator irreversibly withdraw from the cell cycle to initiate fiber cell differentiation, which is coordinated between cyclin, CDKs, and cell-cycle CDKIs.[46] The CDKIs p57$^{Kip2}$ and p27$^{Kip1}$ are highly enriched in newly differentiated fiber cells, suggesting that these factors, which are usually thought to be involved only in cell growth, may also play a role in cell differentiation.[54] For the normal development of the lens, both p57$^{Kip2}$ and p27$^{Kip1}$ are essential, but the CDKI p21$^{Cip1}$ is dispensable.[55] In this study, we found that the loss of lens Znhit1 causes the upregulation of the mRNA and protein levels of both p57$^{Kip2}$ and p21$^{Cip1}$, leading to cell cycle arrest. And sustained cell cycle arrest may result

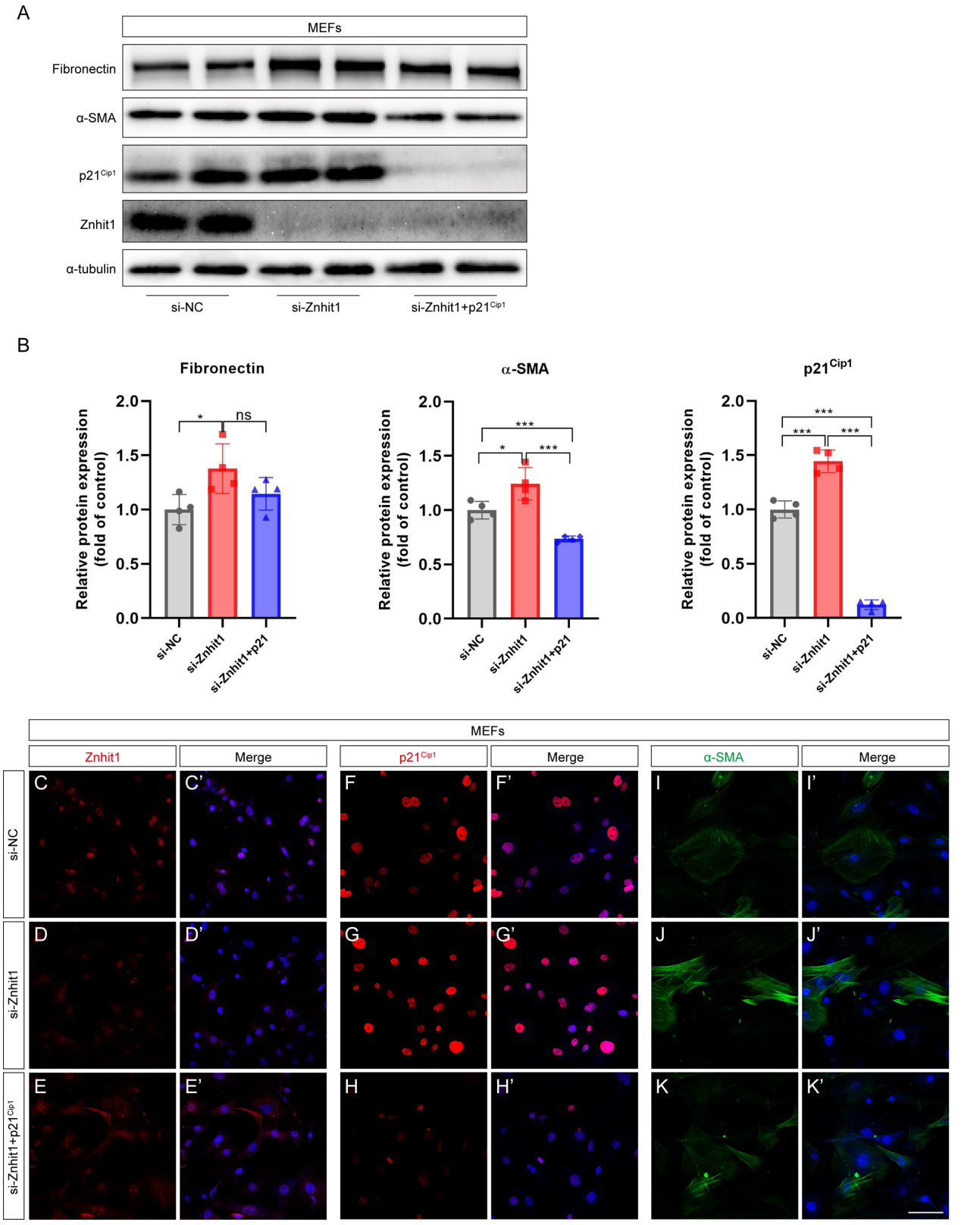


**Figure 10.** Combined knockdown Znhit1 and p21$^{Cip1}$ rescued MEFs transdifferentiation. (**A, B**) MEFs were treated with small interfering control RNA (si-NC), small interfering Znhit1 (si-Znhit1), and si-Znhit+p21$^{Cip1}$ and harvested for western blot analysis of Znhit1, p21$^{Cip1}$, α-SMA and fibronectin expression. α-Tubulin served as the loading control. (**C–K'**) Immunofluorescence showed the expression of Znhit1 (*red*), p21$^{Cip1}$ (*red*), and α-SMA (*green*) in si-NC, si-Znhit1 and si-Znhit1+p21$^{Cip1}$ MEFs. Merge, combined immunolabeled and DAPI-stained images. Scale bars, 100 µm. All values were expressed as means ± standard deviations. Student *t*-test: *$P < 0.05$; ***$P < 0.001$. NC, negative control.

Investigative Ophthalmology & Visual Science

in releasing profibrogenic factors, activating myofibroblasts, eventually leading to fibrosis.[47] However, the expression of $p27^{Kip1}$ was not different between the Znhit1 cKO and control mice. Although $p27^{Kip1}$ expression is normally not required for lens development, it may provide some compensatory function when $p57^{Kip2}$ is absent.[46]

To access the binding of transcription factors, chromatin needs to be modulated by histone modifications and structure remodeling. In this study, the loss of Znhit1 increased the chromatin accessibility of $p57^{Kip2}$ and $p21^{Cip1}$, which elucidates that chromatin accessibility ensures lens fiber cells differentiation. In addition, the loss of Znhit1 also decreased the chromatin accessibility of some genes; these data provided new ideas for researching the signaling pathway of Znhit1-regulated lens development. Further investigations of how Znhit1 to remodel chromatin architecture for lens development are warranted.

Fibrosis is a common pathway to organ injury and malfunction, which is initiated by myofibroblast activation and defined by the accumulation of excess extracellular matrix components. Fibrosis affects nearly every tissue in the body.[56,57] In lens, fibrotic disorders lead to anterior subcapsular cataract and posterior capsule opacification, which can be triggered by aberrant signaling of various molecules, such as TGF-$\beta$, EGF, fibroblast growth factor, and Notch.[58–60] However, how epigenetic regulators and chromatin remodeling complexes regulate lens fibrosis through altering gene expression patterns remains to be determined. Our results showed that the loss of Znhit1 caused lens fibrosis and resulted in organ deformation and dysfunction. The expression of $p21^{Cip1}$ is repressed in normal lens development,[55] but its overexpression leads to Morgagnian globule accumulation and cataract formation in *BubR1*$^{H/H}$ mice.[61] And these features of the Znhit1 cKO lenses are comparable with the defects found in *BubR1*$^{H/H}$ mice. Upregulated $p21^{Cip1}$ expression is a main driver of cell cycle arrest and tissue fibrosis,[62,63] as well as $p27^{Kip1}$.[64,65] However, CDKI it has not been determined whether is $p57^{Kip2}$ associated with fibrosis. In this study, our data demonstrated that the loss of Znhit1 lead to overexpressed $p21^{Cip1}$ and lens fibrosis. Intraperitoneally injected $p21^{Cip1}$ inhibitor rescued Znhit1 cKO-induced fibrosis.

Recent studies had demonstrated that Znhit1 incorporates H2A.Z for stem cell maintenance.[20,21] Breast cancer is the most frequently diagnosed cancer; Znhit1 overexpression inhibited breast cancer tumorigenesis possibly through PTEN-mediated inactivation of the PI3K/Akt/mTOR pathway.[66] These researches explored that Znhit1 could through mediate the incorporation of H2A.Z and the expression of PTEN to exert its function. In this study, we verified that Znhit1 controls lens development by regulating the expression of $p21^{Cip1}$. However, whether Znhit1 modulated the expression of $p21^{Cip1}$ through H2A.Z or PTEN requires additional experiments to be proved.

In conclusion, by applying the cre-loxp approach to generate Znhit1 cKO mice, our study pinpoints a dominant function of Znhit1 in regulating lens differentiation. These Znhit1 cKO–associated changes caused morphological anomalies in lens development, including a decrease in size and vacuolization, the mislocation of lens fiber cell nuclei to the posterior pole, and the disruption of lens fiber cell differentiation. As transcription factors attract increasing attention as viable therapeutic targets,[67] it will be important to elucidate the potential role of Znhit1 in development and diseases.

## Acknowledgments

The authors thank Michael Robinson for the *Mlr10-cre* line, as well as Novogene Bioinformatics Technology Co., Ltd and Shanghai Romics Biotechnology Co., Ltd., for technical assistance.

Supported by Zhejiang Provincial Natural Science Foundation of China under Grant No. LY18C120001.

Author contributions: X.L. and X.Z. supervised the project; J.L. and J.A. conceived and designed the study, and wrote and revised the manuscript. J.L., J.W., X.C., Y.C., C.H., S.J., and D.Y. performed the experiments and analyzed the data. All authors discussed the results and reviewed the manuscript for submission.

Disclosure: **J. Lu,** None; **J. An,** None; **J. Wang,** None; **X. Cao,** None; **Y. Cao,** None; **C. Huang,** None; **S. Jiao,** None; **D. Yan,** None; **X. Lin,** None; **X. Zhou,** None

## References

1. Hejtmancik JF, Shiels A. Overview of the lens. *Prog Mol Biol Transl Sci*. 2015;134:119–127, doi:10.1016/bs.pmbts.2015.04.006.
2. Bassnett S, Šikić H. The lens growth process. *Prog Retin Eye Res*. 2017;60:181–200, doi:10.1016/j.preteyeres.2017.04.001.
3. Bassnett S, Shi Y, Vrensen GFJM. Biological glass: structural determinants of eye lens transparency. *Philos Trans R Soc Lond B Biol Sci*. 2011;366(1568):1250–1264, doi:10.1098/rstb.2010.0302.
4. Hejtmancik JF, Riazuddin SA, McGreal R, Liu W, Cvekl A, Shiels A. Lens biology and biochemistry. *Prog Mol Biol Transl Sci*. 2015;134:169–201, doi:10.1016/bs.pmbts.2015.04.007.
5. Wride MA. Lens fibre cell differentiation and organelle loss: many paths lead to clarity. *Philos Trans R Soc Lond B Biol Sci*. 2011;366(1568):1219–1233, doi:10.1098/rstb.2010.0324.
6. Cvekl A, Ashery-Padan R. The cellular and molecular mechanisms of vertebrate lens development. *Development*. 2014;141(23):4432–4447, doi:10.1242/dev.107953.
7. Griep AE. Cell cycle regulation in the developing lens. *Semin Cell Dev Biol*. 2006;17(6):686–697, doi:10.1016/j.semcdb.2006.10.004.
8. Zhang Z, Wippo CJ, Wal M, Ward E, Korber P, Pugh BF. A packing mechanism for nucleosome organization reconstituted across a eukaryotic genome. *Science*. 2011;332(6032):977–980, doi:10.1126/science.1200508.
9. Hartley PD, Madhani HD. Mechanisms that specify promoter nucleosome location and identity. *Cell*. 2009;137(3):445–458, doi:10.1016/j.cell.2009.02.043.
10. Clapier CR, Cairns BR. The biology of chromatin remodeling complexes. *Annu Rev Biochem*. 2009;78:273–304, doi:10.1146/annurev.biochem.77.062706.153223.
11. Ho L, Crabtree GR. Chromatin remodelling during development. *Nature*. 2010;463(7280):474–484, doi:10.1038/nature08911.
12. Sardiu ME, Cai Y, Jin J, et al. Probabilistic assembly of human protein interaction networks from label-free quantitative proteomics. *Proc Natl Acad Sci USA*. 2008;105(5):1454–1459, doi:10.1073/pnas.0706983105.
13. Cai Y, Jin J, Florens L, et al. The mammalian YL1 protein is a shared subunit of the TRRAP/TIP60 histone acetyltransferase and SRCAP complexes. *J Biol Chem*. 2005;280(14):13665–13670, doi:10.1074/jbc.M500001200.
14. Cuadrado A, Corrado N, Perdiguero E, Lafarga V, Mũoz-Canoves P, Nebreda AR. Essential role of p18Hamlet/SRCAP-mediated histone H2A.Z chromatin

incorporation in muscle differentiation. *EMBO J*. 2010;29(12):2014–2025, doi:10.1038/emboj.2010.85.

15. Hota SK, Bruneau BG. ATP-dependent chromatin remodeling during mammalian development. *Development*. 2016;143(16):2882–2897, doi:10.1242/dev.128892.
16. Sardiu ME, Gilmore JM, Groppe BD, et al. Conserved abundance and topological features in chromatin-remodeling protein interaction networks. *EMBO Rep*. 2015;16(1):116–126, doi:10.15252/embr.201439403.
17. Watanabe S, Radman-Livaja M, Rando OJ, Peterson CL. A histone acetylation switch regulates H2A.Z deposition by the SWR-C remodeling enzyme. *Science*. 2013;340(6129):195–199, doi:10.1126/science.1229758.
18. Dong S, Han J, Chen H, et al. The human SRCAP chromatin remodeling complex promotes DNA-end resection. *Curr Biol*. 2014;24(18):2097–2110, doi:10.1016/j.cub.2014.07.081.
19. Ye B, Liu B, Yang L, et al. Suppression of SRCAP chromatin remodelling complex and restriction of lymphoid lineage commitment by Pcid2. *Nat Commun*. 2017;8(1):1518, doi:10.1038/s41467-017-01788-7.
20. Zhao B, Chen Y, Jiang N, et al. Znhit1 controls intestinal stem cell maintenance by regulating H2A.Z incorporation. *Nat Commun*. 2019;10(1):1071, doi:10.1038/s41467-019-09060-w.
21. Sun S, Jiang N, Jiang Y, et al. Chromatin remodeler Znhit1 preserves hematopoietic stem cell quiescence by determining the accessibility of distal enhancers. *Leukemia*. 2020;34(12):3348–3358, doi:10.1038/s41375-020-0988-5.
22. Maddala R, Chauhan BK, Walker C, et al. Rac1 GTPase-deficient mouse lens exhibits defects in shape, suture formation, fiber cell migration and survival. *Dev Biol*. 2011;360(1):30–43, doi:10.1016/j.ydbio.2011.09.004.
23. Zhao H, Yang Y, Rizo CM, Overbeek PA, Robinson ML. Insertion of a Pax6 consensus binding site into the alphaA-crystallin promoter acts as a lens epithelial cell enhancer in transgenic mice. *Invest Ophthalmol Vis Sci*. 2004;45(6):1930–1939, doi:10.1167/iovs.03-0856.
24. Livak KJ, Schmittgen TD. Analysis of relative gene expression data using real-time quantitative PCR and the 2(-Delta Delta C(T)) Method. *Methods*. 2001;25(4):402–408, doi:10.1006/meth.2001.1262.
25. Lachmann A, Clarke DJB, Torre D, Xie Z, Ma'ayan A. Interoperable RNA-seq analysis in the cloud. *Biochim Biophys Acta Gene Regul Mech*. 2020;1863(6):194521, doi:10.1016/j.bbagrm.2020.194521.
26. Nagaraj N, Wisniewski JR, Geiger T, et al. Deep proteome and transcriptome mapping of a human cancer cell line. *Mol Syst Biol*. 2011;7:548, doi:10.1038/msb.2011.81.
27. Love MI, Huber W, Anders S. Moderated estimation of fold change and dispersion for RNA-seq data with DESeq2. *Genome Biol*. 2014;15(12):550, doi:10.1186/s13059-014-0550-8.
28. Yu G, Wang LG, Han Y, He QY. clusterProfiler: an R package for comparing biological themes among gene clusters. *OMICS*. 2012;16(5):284–287, doi:10.1089/omi.2011.0118.
29. Li H, Durbin R. Fast and accurate short read alignment with Burrows-Wheeler transform. *Bioinformatics*. 2009;25(14):1754–1760, doi:10.1093/bioinformatics/btp324.
30. Zhang Y, Liu T, Meyer CA, et al. Model-based analysis of ChIP-Seq (MACS). *Genome Biol*. 2008;9(9):R137, doi:10.1186/gb-2008-9-9-r137.
31. Heinz S, Benner C, Spann N, et al. Simple combinations of lineage-determining transcription factors prime cis-regulatory elements required for macrophage and B cell identities. *Mol Cell*. 2010;38(4):576–589, doi:10.1016/j.molcel.2010.05.004.
32. Ogino H, Ochi H, Reza HM, Yasuda K. Transcription factors involved in lens development from the preplacodal ectoderm. *Dev Biol*. 2012;363(2):333–347, doi:10.1016/j.ydbio.2012.01.006.
33. Cvekl A, Zhang X. Signaling and gene regulatory networks in mammalian lens development. *Trends Genet*. 2017;33(10):677–702, doi:10.1016/j.tig.2017.08.001.
34. Wilson A, Laurenti E, Oser G, et al. Hematopoietic stem cells reversibly switch from dormancy to self-renewal during homeostasis and repair. *Cell*. 2008;135(6):1118–1129, doi:10.1016/j.cell.2008.10.048.
35. Audette DS, Anand D, So T, et al. Prox1 and fibroblast growth factor receptors form a novel regulatory loop controlling lens fiber differentiation and gene expression. *Development*. 2016;143(2):318–328, doi:10.1242/dev.127860.
36. Ashery-Padan R, Marquardt T, Zhou X, Gruss P. Pax6 activity in the lens primordium is required for lens formation and for correct placement of a single retina in the eye. *Genes Dev*. 2000;14(21):2701–2711, doi:10.1101/gad.184000.
37. Shinde A V, Humeres C, Frangogiannis NG. The role of $\alpha$-smooth muscle actin in fibroblast-mediated matrix contraction and remodeling. *Biochim Biophys Acta Mol Basis Dis*. 2017;1863(1):298–309, doi:10.1016/j.bbadis.2016.11.006.
38. Poli J, Gasser SM, Papamichos-Chronakis M. The INO80 remodeller in transcription, replication and repair. *Philos Trans R Soc Lond B Biol Sci*. 2017;372(1731):20160290, doi:10.1098/rstb.2016.0290.
39. Klemm SL, Shipony Z, Greenleaf WJ. Chromatin accessibility and the regulatory epigenome. *Nat Rev Genet*. 2019;20(4):207–220, doi:10.1038/s41576-018-0089-8.
40. Willhoft O, Wigley DB. INO80 and SWR1 complexes: the non-identical twins of chromatin remodelling. *Curr Opin Struct Biol*. 2020;61:50–58, doi:10.1016/j.sbi.2019.09.002.
41. Morse RH. Transcription factor access to promoter elements. *J Cell Biochem*. 2007;102(3):560–570, doi:10.1002/jcb.21493.
42. Phillips JE, Corces VG. CTCF: master weaver of the genome. *Cell*. 2009;137(7):1194–1211, doi:10.1016/j.cell.2009.06.001.
43. Arzate-Mejía RG, Recillas-Targa F, Corces VG. Developing in 3D: the role of CTCF in cell differentiation. *Development*. 2018;145(6):dev137729, doi:10.1242/dev.137729.
44. Beishline K, Azizkhan-Clifford J. Sp1 and the 'hallmarks of cancer'. *FEBS J*. 2015;282(2):224–258, doi:10.1111/febs.13148.
45. Innocente SA, Lee JM. p53 is a NF-Y- and p21-independent, Sp1-dependent repressor of cyclin B1 transcription. *FEBS Lett*. 2005;579(5):1001–1007, doi:10.1016/j.febslet.2004.12.073.
46. Zhang P, Wong C, DePinho RA, Harper JW, Elledge SJ. Cooperation between the Cdk inhibitors p27(KIP1) and p57(KIP2) in the control of tissue growth and development. *Genes Dev*. 1998;12(20):3162–3167, doi:10.1101/gad.12.20.3162.
47. Wang W, Sun W, Gao B, Lian X, Zhou H. Cell cycle arrest as a therapeutic target of acute kidney injury. *Curr Protein Pept Sci*. 2017;18(12):1224–1231, doi:10.2174/1389203717666160915162238.
48. Lovisa S, LeBleu VS, Tampe B, et al. Epithelial-to-mesenchymal transition induces cell cycle arrest and parenchymal damage in renal fibrosis. *Nat Med*. 2015;21(9):998–1009, doi:10.1038/nm.3902.
49. Yang L, Besschetnova TY, Brooks CR, Shah J V., Bonventre J V. Epithelial cell cycle arrest in G2/M mediates kidney fibrosis after injury. *Nat Med*. 2010;16(5):535–543, doi:10.1038/nm.2144.
50. Oshima T, Fujiu K. Cell cycle arrest-driven fibrosis. *Int Heart J*. 2019;60(4):785–787, doi:10.1536/ihj.19-293.

Investigative Ophthalmology & Visual Science

51. Wettersten HI, Hwang SH, Li C, et al. A novel p21 attenuator which is structurally related to sorafenib. *Cancer Biol Ther*. 2013;14(3):278–285, doi:10.4161/cbt.23374.
52. Kumar B, Reilly MA. The development, growth, and regeneration of the crystalline lens: a review. *Curr Eye Res*. 2020;45(3):313–326, doi:10.1080/02713683.2019.1681003.
53. wei Gao S, F Liu. Novel insights into cell cycle regulation of cell fate determination. *J Zhejiang Univ Sci B*. 2019;20(6):467–475, doi:10.1631/jzus.B1900197.
54. Lovicu FJ, McAvoy JW. Spatial and temporal expression of p57(KIP2) during murine lens development. *Mech Dev*. 1999;86(1–2):165–169, doi:10.1016/s0925-4773(99)00106-9.
55. Tateishi Y, Matsumoto A, Kanie T, Hara E, Nakayama K, Nakayama KI. Development of mice without Cip/Kip CDK inhibitors. *Biochem Biophys Res Commun*. 2012;427(2):285–292, doi:10.1016/j.bbrc.2012.09.041.
56. Rockey DC, Bell PD, Hill JA. Fibrosis – a common pathway to organ injury and failure. *N Engl J Med*. 2015;372(12):1138–1149, doi:10.1056/nejmra1300575.
57. Hinz B. Myofibroblasts. *Exp Eye Res*. 2016;142:56–70, doi:10.1016/j.exer.2015.07.009.
58. Chen X, Yan H, Chen Y, Li G, Bin Y, Zhou X. Moderate oxidative stress promotes epithelial-mesenchymal transition in the lens epithelial cells via the TGF-$\beta$/Smad and Wnt/$\beta$-catenin pathways. *Mol Cell Biochem*. 2021;476(3):1631–1642, doi:10.1007/s11010-020-04034-9.
59. Eldred JA, Dawes LJ, Wormstone IM. The lens as a model for fibrotic disease. *Philos Trans R Soc Lond B Biol Sci*. 2011;366(1568):1301–1319, doi:10.1098/rstb.2010.0341.
60. Lovicu FJ, Shin EH, McAvoy JW. Fibrosis in the lens. Sprouty regulation of TGF$\beta$-signaling prevents lens EMT leading to cataract. *Exp Eye Res*. 2016;142:92–101, doi:10.1016/j.exer.2015.02.004.
61. Baker DJ, Weaver RL, van Deursen JM. p21 both attenuates and drives senescence and aging in BubR1 progeroid mice. *Cell Rep*. 2013;3(4):1164–1174, doi:10.1016/j.celrep.2013.03.028.
62. Hernandez-Segura A, Nehme J, Demaria M. Hallmarks of cellular senescence. *Trends Cell Biol*. 2018;28(6):436–453, doi:10.1016/j.tcb.2018.02.001.
63. Yosef R, Pilpel N, Papismadov N, et al. p21 maintains senescent cell viability under persistent DNA damage response by restraining JNK and caspase signaling. *EMBO J*. 2017;36(15):2280–2295, doi:10.15252/embj.201695553.
64. Das S, Neelamegam K, Peters WN, Periyasamy R, Pandey KN. Depletion of cyclic-GMP levels and inhibition of cGMP-dependent protein kinase activate p21Cip1/p27Kip1 pathways and lead to renal fibrosis and dysfunction. *FASEB J*. 2020;34(9):11925–11943, doi:10.1096/fj.202000754R.
65. Fujigaki Y, Sun D, Fujimoto T, et al. Cytokines and cell cycle regulation in the fibrous progression of crescent formation in antiglomerular basement membrane nephritis of WKY rats. *Virchow Arch*. 2001;439(1):35–45, doi:10.1007/s004280100433.
66. Cui C, Li S, Wu D. Znhit1 inhibits breast cancer by up-regulating PTEN to deactivate the PI3K/Akt/mTOR pathway. *Life Sci*. 2019;224:204–211, doi:10.1016/j.lfs.2019.03.067.
67. Hishikawa A, Hayashi K, Itoh H. Transcription factors as therapeutic targets in chronic kidney disease. *Molecules*. 2018;23(5):1123, doi:10.3390/molecules23051123.